

Magnetic structure of the *kagomé* lattice antiferromagnet potassium jarosite $\text{KFe}_3(\text{OH})_6(\text{SO}_4)_2$

T. Inami*

Japan Atomic Energy Research Institute, Tokai, Ibaraki 319-11, Japan

M. Nishiyama and S. Maegawa

Graduate School of Human and Environmental Studies, Kyoto University, Kyoto 606-8501, Japan

Y. Oka

Faculty of Integrated Human Studies, Kyoto University, Kyoto 606-8501, Japan

(Received 27 August 1999; revised manuscript received 29 November 1999)

We have examined the magnetic structure of the *kagomé* lattice antiferromagnet potassium jarosite (K jarosite: $\text{KFe}_3(\text{OH})_6(\text{SO}_4)_2$) by means of powder neutron diffraction. Extremely high degeneracy of the ground states prevents the long-range magnetic ordering at any temperature and the $\sqrt{3} \times \sqrt{3}$ structure is predicted theoretically to be favored rather than the $q=0$ structure at $T=0$ in a *kagomé* lattice Heisenberg antiferromagnet. Nevertheless, K jarosite shows long-range magnetic ordering at 65 K and the ordered magnetic structure was found to be the $q=0$ structure. In addition, although the $q=0$ structure has two degenerated states of “positive” and “negative” chirality, the observed magnetic structure contains only elemental triangles of positive chirality. We found that a weak single-ion-type anisotropy is crucial for selecting the observed magnetic structure. The long-range magnetic ordering at finite temperature in the jarosite family of compounds can be ascribed to this anisotropy.

I. INTRODUCTION

Magnetically frustrated systems, particularly in which the frustration is caused by mainly the geometry of the lattice, have been a subject of recent intensive experimental and theoretical works.¹ A *kagomé* lattice is an example of those lattices, which are commonly composed of triangles of antiferromagnetic interactions. The ground-state properties of spins on the *kagomé* lattice coupled to each other via nearest-neighbor antiferromagnetic interaction have been a long-standing theoretical issue. Especially, the *kagomé* lattice antiferromagnet of classical Heisenberg spins has a large number of degenerated ground states and hence does not develop long-range order (LRO) at any temperatures. Instead, novel ground states are expected as $T \rightarrow 0$.^{2,3}

Several perturbations, such as further-neighbor interactions,⁴ lattice disorder,⁵ and anisotropy,⁶ which are usually encountered in a real magnet, can lift such degeneracy of the ground state, and may cause long-range magnetic ordering. The jarosite family of compounds $A\text{Fe}_3(\text{OH})_6(\text{SO}_4)_2$ ($A = \text{H}_3\text{O}, \text{Na}, \text{K}, \text{NH}_4, \text{Rb}, \text{Tl}, \text{Ag}$) has the *kagomé* lattice in the crystal structure, as shown in Fig. 1 for K jarosite. The magnetic ion Fe^{3+} , which is centered in an oxygen octahedron, is well approximated by a classical Heisenberg spin with $S = 5/2$ and forms a *kagomé* lattice in the *ab* plane, which is widely separated from an adjacent *kagomé* plane by nonmagnetic A^+ and SO_4^{2-} ions. The magnetic susceptibility has been measured and was found to follow a Curie-Weiss law with negative Weiss temperature $\Theta \sim -700$ K,⁷⁻⁹ indicating a major interaction between the spins is antiferromagnetic. Therefore, jarosites are expected to be a good model of a two-dimensional Heisenberg *kagomé* lattice antiferromagnet. However, most of jarosites have magnetic LRO below $T_N \sim 60$ K.⁷⁻¹⁰ Although the small val-

ues of $T_N/\Theta \sim 0.1$ show a large degree of frustration, deviation from an ideal Heisenberg *kagomé* lattice antiferromagnet must be present and induce the LRO in these magnets.

In this paper, we measured magnetic susceptibility and powder neutron-diffraction patterns of K jarosite. Neutron-diffraction measurement of K jarosite has been made before by Townsend *et al.*⁸ They, however, appears to have failed to determine a correct ordering pattern.¹⁰ We obtained a reasonable magnetic structure with respect to the spin configuration between the *kagomé* planes from the neutron data. The obtained magnetic structure is the so-called $q=0$ type 120°

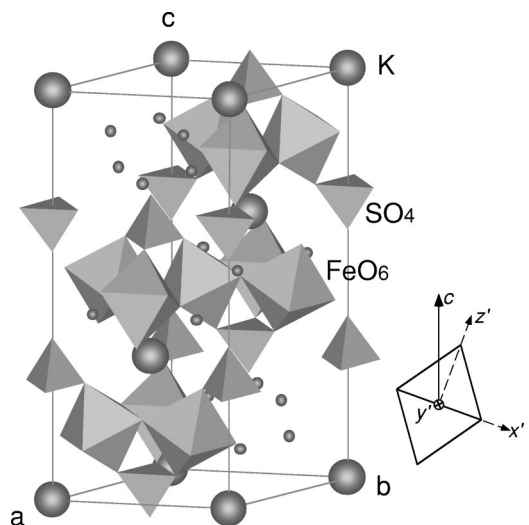


FIG. 1. Crystal structure of K jarosite. The FeO_6 octahedra and SO_4 tetrahedra are shaded. The K and H sites are shown as large and small spheres, respectively. The inclined FeO_6 octahedron and the local coordinate (x' , y' and z') on the Fe^{3+} ion are also shown.

spin structure in the ab plane. The $q=0$ structure is usually doubly degenerated due to the direction in which the spins turn, clockwise or counterclockwise. However, the $q=0$ structure observed in K jarosite was found to possess only triangles on which the spins turn clockwise. We introduce weak single-ion-type anisotropy by considering local symmetry of the Fe site in order to explain the observed unusual feature of the magnetic structure and will show importance of the anisotropy on the ordering in K jarosite.

II. EXPERIMENTAL

Two powder specimens (K jarosite 1 and deuterated 2) were obtained by hydrothermal treatment. The K jarosite 1 was synthesized by reacting $\text{Fe}_2(\text{SO}_4)_3\text{-K}_2(\text{SO}_4)$ solution at 200 °C for 56 h sealed in a Pyrex ampule using an autoclave. The obtained precipitation was washed with hot water and dried. For reducing large incoherent background from proton in neutron diffraction measurements, the deuterated K jarosite 2 was prepared in the same manner as sample 1 at 180 °C for 36 h using 99.75% D_2O . $\text{Fe}_2(\text{SO}_4)_3$ dehydrated at 400 °C for 3 h was used in order to avoid contamination of hydrogen. X-ray powder-diffraction analysis showed that the products were single phase. Typical dimension of the sample 1 was about 5–20 μm from SEM observation.

The susceptibility was measured with increasing temperature from 2 to 300 K under a magnetic field 500 Oe using a superconducting quantum interference device magnetometer (Quantum Design: MPMS2). Due to a small amount of paramagnetic impurity, the susceptibility tends to diverge toward 0 K. We extracted the impurity part as below. The magnetization curves were measured up to 5 T at several temperatures and were divided into two parts; magnetization which is linear in magnetic field and one which follows the Brillouin function. The latter component was associated with impurities and was subtracted from the observed susceptibility.

Neutron-diffraction measurements were performed on the high-resolution powder diffractometer HRPD and the triple-axis spectrometer TAS-2 installed at the research reactor JRR-3M, JAERI (Tokai). The powder neutron-diffraction pattern of sample 1 was collected on HRPD at 10 K from 5 to 165° in 2θ with a wave length 1.823 Å. Neutron-diffraction patterns of sample 2 were measured on TAS-2 at temperatures 7 and 100 K from 15 to 85° in 2θ with a wave length 2.365 Å. The temperature dependence of magnetic Bragg reflections was measured on TAS-2 with the two-axis mode. Samples 1 and 2 were contained in cylindrical vanadium cans with ^4He exchange gas with diameters of 6 and 10 mm, respectively, and cooled by a conventional ^4He closed-cycle refrigerator. All diffraction pattern were analyzed using the Rietveld refinement program RIETAN.^{10,11} In the refinements, the background was fitted with a 12-term polynomial (sample 1) and a nine-term polynomial (sample 2) and a pseudo-Voigt peak shape function was employed. The magnetic form factor of Fe^{3+} was used to calculate the magnetic scattering amplitude.

III. RESULTS

The susceptibility of samples 1 and 2, of which the impurity part was subtracted, is depicted in Fig. 2. Above 100 K

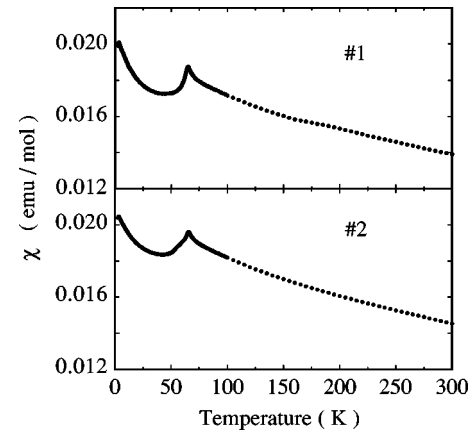


FIG. 2. Magnetic susceptibility of K jarosite 1 and 2.

the susceptibility appears to follow a Curie-Weiss law. Obtained Weiss temperatures and Curie constants are listed in Table I. The Weiss temperatures are of the order of -700 K, implying a large antiferromagnetic interaction between the spins. Since the absolute values of the Weiss temperatures exceed the measured temperature range, a Curie-Weiss law may not be applicable. Harris *et al.* calculated the uniform susceptibility χ_0 of a *kagomé* lattice using high-temperature expansions.⁴ They showed that χ_0 deviates from the Curie-Weiss law due to the short-range correlation and is expressed at low temperatures as the corrected Curie-Weiss law

$$\chi_0 = \frac{C'}{T + \Theta'}, \quad (1)$$

where $C' = \frac{9}{8}C$, $\Theta' = \frac{3}{2}\Theta$, and C and Θ are conventional Curie constant and Weiss temperature, respectively. If the nearest-neighbor interaction in the *kagomé* plane is dominant, the exchange constant J is estimated to be about -20 K from $\Theta = 2zJS(S+1)/3$ where $z=4$. The effective Bohr magnetons μ_{eff} were evaluated to be 6.0 ± 0.2 and $5.9 \pm 0.1 \mu_B$ for samples 1 and 2, respectively, using $C = N\mu_{\text{eff}}^2/3k_B$ where $\mu_{\text{eff}} = g\mu_B\sqrt{S(S+1)}$, and are in good accordance with the free-ion value $5.92 \mu_B$ ($g=2$). This assures that the occupancy of the Fe site is close to unity, $103 \pm 7\%$ (sample 1) and $100 \pm 3\%$ (sample 2). A single cusp was observed at 65 K for both samples and is considered to be the appearance of the long-range magnetic order as will be shown later in neutron-diffraction measurements.

Figure 3 shows the observed, calculated and difference neutron powder-diffraction patterns for sample 1 measured at 10 K. We only measured magnetically ordered phase, because nuclear and magnetic Bragg peaks have already been assigned in the previous measurements.^{8,10} The background

TABLE I. Curie constants (C') and Weiss temperatures (Θ') deduced from the magnetic susceptibility using Harris's corrected Curie-Weiss law. Effective Bohr magnetons (μ_{eff}) were evaluated from $C' = 9/8 C$ and $C = N\mu_{\text{eff}}^2/3k_B$. See text.

	C' /(emu K/mol)	Θ' /K	μ_{eff}/μ_B
1	15.3(7)	-800(50)	6.0(2)
2	14.8(5)	-720(30)	5.9(1)

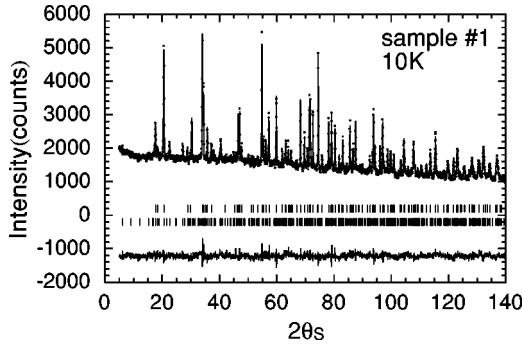


FIG. 3. Observed (dots) and calculated (solid line) neutron-diffraction profiles of K jarosite 1 at 10 K. The difference is shown below. Reflection positions are marked for nuclear reflections (upper) and magnetic reflections (lower).

was very high owing to the strong incoherent scattering from proton. Refinement was performed for nuclear and magnetic structure simultaneously. The determination of the magnetic structure will be described later. For the refinement of the nuclear structure, we used the atomic coordinates in Ref. 8 as initial parameters. The space group of the crystal structure is $R\bar{3}m$. The occupation factors of K and Fe sites were free, because the partial substitution of H_3O^+ for K^+ and vacancies of the Fe sites have been reported for jarosites.^{8,12} The refinement readily converged to $R_{wp}=3.87\%$. The deduced parameters and selected bond lengths are summarized in Table II. The obtained occupancy at the Fe site is very high

($99 \pm 1\%$) and agrees with the susceptibility result mentioned above, while there seems to be a medium deficiency at the K site.

The magnetic structure was determined as follows. The diffraction patterns of the deuterated sample 2 measured at 100 and 7 K are shown in Fig. 4. A quite low background indicates that almost complete substitution of deuteron for proton and this is of great advantage to estimate magnetic intensity. The magnetic reflections could be indexed using hexagonal setting as shown in Fig. 4(b). There is an apparent extinction rule that $h-k+2l=3n$ (n : integer), hence the space group is found to belong to rhombohedral one. The magnetic unit cell is twice as large as the nuclear one along the c axis and contains independent six spins. However, since the magnetic reflections are observed only at $hkl/2$ (l : odd integer), the spin at (x,y,z) is antiparallel to one at $(x,y,z+1)$, thus only three spins are truly independent in the unit cell. Here we employed the 120° structure because the nearest-neighbor interaction between the spins is antiferromagnetic. This is the so-called $q=0$ structure for a *kagomé* lattice antiferromagnet. There are two possibilities for spin configuration depending on the chirality as shown in Figs. 5(a) and 5(b). The chiral vector \mathbf{n} is defined as

$$\mathbf{n} = \left(\frac{2}{3\sqrt{3}} \right) (\mathbf{S}_1 \times \mathbf{S}_2 + \mathbf{S}_2 \times \mathbf{S}_3 + \mathbf{S}_3 \times \mathbf{S}_1), \quad (2)$$

where \mathbf{S}_1 , \mathbf{S}_2 , and \mathbf{S}_3 are spins on the vertices of an elementary triangle. When the three spins form a coplanar 120°

TABLE II. Crystallographic and magnetic data and selected bond lengths deduced from Rietveld refinements for K jarosite 1 (10 K) and deuterated K jarosite 2 (7 K).

Sample 1		$a=7.2999(3) \text{ \AA}$, $c=17.1157(5) \text{ \AA}$				
		$R_{wp}=3.87\%$, $R_{exp}=2.49\%$, $R_F=7.12\%$, $R_M=11.05\%$				
		Occupancy	x	y	z	B_{iso}/A^2
K	$3a$	0.93(3)	0.0	0.0	0.0	0.7(3)
Fe	$9d$	0.99(1)	0.5	0.5	0.5	0.43(9)
S	$6c$	1.0	0.0	0.0	0.3092(7)	0.6(2)
O(1)	$6c$	1.0	0.0	0.0	0.3941(3)	0.2(1)
O(2)	$18h$	1.0	0.2227(2)	-0.2227	-0.0534(2)	0.51(8)
H	$18h$	1.0	0.1953(4)	-0.1953	0.1106(3)	1.5(1)
O(3)	$18h$	1.0	0.1287(2)	-0.1287	0.1349(2)	0.52(8)
Fe-O(2)	$\times 2$		2.065(3) \AA		μ_{Fe}/μ_B	3.80(6)
Fe-O(3)	$\times 4$		1.989(1) \AA			
O(3)-O(3)	$\times 2$		2.806(3) \AA			
		$\times 2$	2.819(5) \AA			
Sample 2		$a=7.3013(8) \text{ \AA}$, $c=17.097(1) \text{ \AA}$				
		$R_{wp}=6.45\%$, $R_{exp}=3.72\%$, $R_F=1.17\%$, $R_M=1.38\%$				
		Occupancy	x	y	z	B_{iso}/A^2
K	$3a$	1.0	0.0	0.0	0.0	0.1
Fe	$9d$	1.0	0.5	0.5	0.5	0.1
S	$6c$	1.0	0.0	0.0	0.311(1)	0.1
O(1)	$6c$	1.0	0.0	0.0	0.3941(6)	0.3
O(2)	$18h$	1.0	0.2238(4)	-0.2238	-0.0534(3)	0.3
D	$18h$	1.0	0.1957(4)	-0.1957	0.1106(3)	1.0
O(3)	$18h$	1.0	0.1286(4)	-0.1286	0.1361(4)	0.3
					μ_{Fe}/μ_B	3.80(3)

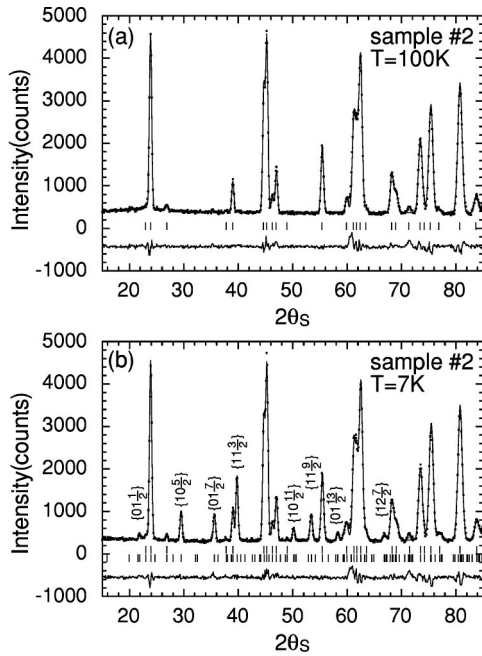


FIG. 4. Observed, calculated and difference neutron-diffraction profiles of deuterated K jarosite 2, at (a) 100 K and (b) 7 K. Vertical ticks indicate the positions of nuclear [(a) and upper row in (b)] and magnetic [lower row in (b)] Bragg reflections. Magnetic reflections are indexed in (b). The lower ticks in (b) are generated using space group $\bar{1}$.

structure, the normal component of \mathbf{n} to the spin plane has the largest (or smallest) value $+1$ (or -1). Here we follow the convention that the chirality is $+1$ when the spins rotate clockwise by 120° as one traverses around the triangle clockwise. We calculated magnetic structure factors of models (a) and (b) with varying ϕ by a 30° step for two cases that the spins are in the ab and ac plane. Interestingly, while the structure factor is a function of ϕ for the model (a), it is independent of ϕ for the model (b). The good agreement was

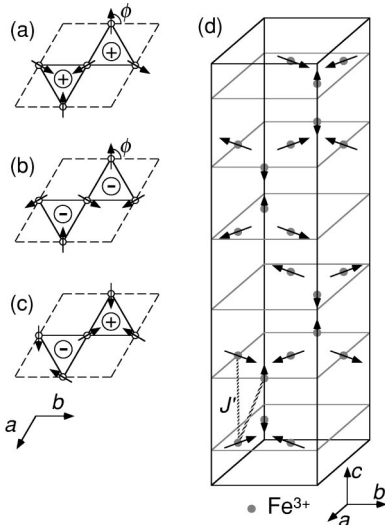


FIG. 5. (a) $q=0$ structure with $+1$ chirality, (b) $q=0$ structure with -1 chirality, (c) $\sqrt{3}\times\sqrt{3}$ structure, and (d) the best model of the magnetic structure for K jarosite. The plus and minus signs indicate the chirality of the triangle of the spins.

obtained for the model (a) at $\phi=90^\circ$ (and -90°) with the spins in the ab plane. It should be noted that only this model can reproduce a remarkable feature in the diffraction pattern that the observed intensity of $01\frac{1}{2}$ is very weak. Model (a) with $\phi\neq 90^\circ$ and model (b) result in much larger intensity at $01\frac{1}{2}$. Refinement using this model successfully converged to $R_{wp}=6.45\%$. The results are also summarized in Table II and the obtained magnetic structure is shown in Fig. 5(d). All occupancy factors and thermal parameters of sample 2 were fixed during the refinement, because the measured range of 2θ is too small to reliably extract those parameters. The same model of the magnetic structure was applied in the refinement of sample 1. The spin configuration between the *kagomé* planes is easily understood; a nearest-neighbor ferromagnetic coupling between the spins on adjacent planes [J' in Fig. 5(d)] simply leads to our magnetic structure.¹³ The magnitude of the ordered moments per Fe^{3+} ion was evaluated from the refinements to be $3.80(6)$ and $3.80(3)\mu_B$ for samples 1 and 2, respectively.

The peak intensities of the magnetic reflections, shown as a function of temperature in Fig. 6, decrease monotonically with increasing temperature with similar way. The ordering temperatures of samples 1 and 2 are estimated to be 67 ± 1 K and 65 ± 1 K, respectively. Since the temperatures at which the cusps are observed in the susceptibility are in good agreement with the temperatures at which the magnetic Bragg peaks disappear, those anomalies in the susceptibility can be ascribed to the onset of the long-range magnetic ordering. For the sample 2, we show temperature dependence of three magnetic reflections $01\frac{7}{2}$, $10\frac{5}{2}$, and $11\frac{3}{2}$. These intensities are normalized at 10 K and decrease as almost the same manner with increasing temperature. Thus the ratios between the three reflections are almost constant over the measured temperature range, hence it turns out that there is no notable change in magnetic structure in the ordered phase.

In the last part of this section, we mention sample dependence in K jarosite. Two anomalies in the magnetic susceptibility for K, Na, and NH_4 jarosites were reported previously, and combined with the NMR results, successive phase transitions in these compounds were concluded.⁹ However, the newly synthesized samples in the present study show a single cusp in the susceptibility. For jarosite-type compounds, a deficiency in the alkaline and transition-metal sites is reported, and the degree of the deficiency depends on preparation condition.¹² The magnetic properties may depend on those deficiencies. Within the accuracy of the Rietveld refinements, however, no significant difference was observed in occupancy factors between the previous sample and present ones. In addition, there is no clear difference in the ordered magnetic structure and in the temperature dependence of the magnetic Bragg peaks. Although the susceptibility behaved really differently between the samples near T_N (probably due to the deficiency), magnetic properties well below T_N are considered to be insensitive to preparation condition.

IV. DISCUSSION

As seen in the previous section, the ordered magnetic structure has the quite specific features and gives us fruitful

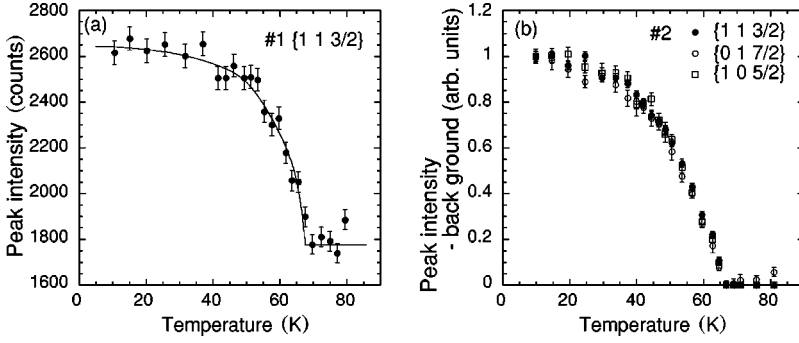


FIG. 6. Temperature dependence of magnetic Bragg peaks, (a) sample 1 and (b) sample 2. The solid line in (a) is a guide to the eye.

information about magnetic property of K jarosite. We found that the magnetic structure consists of *only* triangles of the spins which have +1 chirality [model (a) in Fig. 5]. This is a rather surprising result, because the ground-state energy of the $q=0$ structure with +1 chirality [Fig. 5(a)] is equal to that with -1 chirality [Fig. 5(b)] if only the Heisenberg interaction between the spins is considered. Moreover, the direction of the ordered moments is fixed. All spins point to or away from the center of the triangle. It must be stressed that only the spin configuration in Fig. 5(d) and the reversed one are selected in K jarosite. Such a result could not be explained without taking into account an anisotropy which has an inplane component.

This can be understood if one is aware of the fact that there is no trigonal symmetry at the Fe site. The site symmetry is $2/m$. The Fe^{3+} ion is surrounded by four oxygens [O(3)] of the OH^- ions and two oxygens [O(2)] of the SO_4^{2-} ions. This octahedron is elongated along the O(2) oxygens, and the four O(3) oxygens form a rectangle. Thus the spin Hamiltonian is described as

$$\mathcal{H} = -2J \sum_{\langle i,j \rangle} \mathbf{S}_i \cdot \mathbf{S}_j - D \sum_i (S_i^{z'})^2 - E \sum_i \{(S_i^{x'})^2 - (S_i^{y'})^2\}, \quad (3)$$

where the z' and y' -axes are taken to be parallel to O(2)-Fe-O(2) and to be in the ab plane for each Fe^{3+} ion, respectively. The x' axis is perpendicular to the both axes (see Fig. 1). A stable magnetic structure stems from competition between the nearest-neighbor interaction J and the single-ion-type anisotropies D and E . It is thought that D is negative (easy-plane type) because the ordered moments were found to lie (almost) in the ab plane. The antiferromagnetic interaction J prefers a coplanar 120° structure. Consider first that E is negative. In this case, the magnetic moment tends to be parallel to the y' axis, thus the coplanar structure of +1 chirality [Fig. 5(a)] with $\phi=0$ or 180° gives the lowest energy. Note that requirements from D , E , and J are all satisfied, hence the 120° structure is truly coplanar. When $E > 0$, the magnetic moment tends to be parallel to the x' axis. However, the x' axes are not in the same plane, thus the anisotropy competes with J . Since it is thought that $|J| \gg |D|$ and $|E|$, the resultant magnetic structure is predominantly coplanar. If E is large enough, the $q=0$ structure of +1 chirality with $\phi=90$ or -90° is selected. This is the magnetic structure observed in K jarosite. The spins on the triangle slightly cant from a coplanar structure like an umbrella in order to partly satisfy E .

As a result, it is found that the reason only the $q=0$ structure with +1 chirality is selected is that the symmetry of the magnetic structure in K jarosite is the same as the crystallographic one. This is shown by the fact that the model (a) has the threefold axis but the model (b) does not. In addition, it may also explain why the $q=0$ in-plane structure is realized in K jarosite instead of the $\sqrt{3} \times \sqrt{3}$ structure. As seen in Fig. 5, the $q=0$ structure contains triangles with only +1 (or -1) chirality, while the $\sqrt{3} \times \sqrt{3}$ structure consists of both triangles with +1 and -1 chirality. Therefore, the $\sqrt{3} \times \sqrt{3}$ structure cannot satisfy the single-ion-type anisotropy as the $q=0$ structure with +1 chirality does. Some interplane or second- and third-neighbor in-plane interactions make the $q=0$ structure preferable to the $\sqrt{3} \times \sqrt{3}$ structure.^{4,13} However, these isotropic interactions do not explain the observed spin structure, which has only +1 chirality and fixed spin directions. Consequently, our results clearly indicate that the Fe^{3+} ions in K jarosite have a weak single-ion-type anisotropy and that it plays an important role for selecting the observed magnetic structure. It is interesting to note that the umbrella structure of the spins results in a net moment for each *kagomé* plane. The net moment stacks in an antiparallel manner layer by layer, thus no bulk moment appears in K jarosite. If it accumulates ferromagnetically, a weak ferromagnetic moment must be observed. Actually the chromate analog $\text{KFe}_3(\text{OH})_6(\text{CrO}_4)_2$, which has a magnetic structure consistent with the ferromagnetic stacking of the net moments, was found to show a spontaneous moment.⁸ This fact supports the existence of a canted umbrella of spins in jarosites.

Irrespective of the system being quantum or classical, it is considered that Heisenberg spins on a two-dimensional *kagomé* lattice coupled antiferromagnetically to each other do not show LRO. Hence a real *kagomé* lattice antiferromagnet which has the LRO must have some deviation from an ideal one. Usually the first candidate is an interplane coupling, because a real system is inevitably three-dimensional (3D). In fact, in K jarosite the 3D ordering pattern manifests the ferromagnetic coupling between the spins on the adjacent planes as mentioned in the previous section.¹³ However, interplane distance in K jarosite is rather large (~ 5.7 Å) and available superexchange paths contain more than four bonds, thus interplane interactions are thought to be very small and are not considered as the main cause of the 3D LRO.

As the second candidate, Wills *et al.* proposed that structural disorder is essential for magnetic LRO of jarosites.^{12,14,15} They mentioned that hydronium-jarosite $(\text{H}_3\text{O})\text{Fe}_3(\text{OH})_6(\text{SO}_4)_2$ had least disorder among jarosites and

did not show a magnetic LRO down to 2 K. On the contrary to this, they found that magnetically diluted hydronium-jarosite showed magnetic LRO at 25.5 K.¹⁵ Their idea is, thus, that vacancy at the Fe site lifts the degeneracy of ground states and induces the LRO in that system. According to this, they also ascribed rather high Néel temperature of other jarosites to incomplete occupation of the Fe site. This scenario is fascinating; if one succeeded in making chemically perfect jarosite, it might not show any magnetic ordering down to 0 K.

However, we believe the third candidate, anisotropy, is most important in K jarosite. As we showed above, the peculiar features of the observed magnetic structure were only explained by taking into account a weak single-ion-type anisotropy, and the existence of the D and E terms in the spin Hamiltonian is understood straightforwardly from the crystallographic consideration. Due to this anisotropy, allowed configurations are only two, model (a) in Fig. 5 with $\phi = 90$ and -90° . This is equivalent to describing the magnetic moments in the K jarosite as effectively having an Ising in-plane anisotropy. Limited configurations illustrate that the

Ising anisotropy suppresses the magnetic fluctuations, which are specific to a *kagomé* lattice antiferromagnet. Hence we think that K jarosite behaves like a two-dimensional Ising antiferromagnet, which has LRO at a finite temperature, rather than a Heisenberg *kagomé* lattice antiferromagnet.

In conclusion, we have investigated the magnetic structure of K jarosite from the neutron powder-diffraction measurements. From the observed magnetic structure we deduced the fact that the single-ion-type anisotropy governs magnetic order in K jarosite. We think that the finite ordering temperature of K jarosite should be ascribed to the Ising anisotropy, which lifts the degeneracy of the ground states.

ACKNOWLEDGMENTS

The authors wish to acknowledge helpful discussions with Professor K. Kubo and would like to thank Y. Shimojo for his technical support on neutron-scattering experiments. We are also grateful to Dr. F. Izumi for permitting us to modify his Rietveld refinement program RIETAN.

*Present address: Department of Synchrotron Radiation Research, Japan Atomic Energy Research Institute, Mikazuki, Hyogo 679-5148, Japan.

¹P. Schiffer and A. P. Ramirez, *Comments Condens. Matter Phys.* **18**, 21 (1996), and references therein.

²J. N. Reimers and A. J. Berlinsky, *Phys. Rev. B* **48**, 9539 (1993).

³J. T. Chalker, P. C. W. Holdsworth, and E. F. Shender, *Phys. Rev. Lett.* **68**, 855 (1992).

⁴A. B. Harris, C. Kallin, and A. J. Berlinsky, *Phys. Rev. B* **45**, 2899 (1992).

⁵C. L. Henley, *Phys. Rev. Lett.* **62**, 2056 (1989).

⁶A. Kuroda and S. Miyashita, *J. Phys. Soc. Jpn.* **64**, 4509 (1995).

⁷M. Takano, T. Shinjyo, and T. Takada, *J. Phys. Soc. Jpn.* **30**, 1049 (1971).

⁸M. G. Townsend, G. Longworth, and E. Roudaut, *Phys. Rev. B*

33, 4919 (1986).

⁹S. Maegawa, M. Nishiyama, N. Tanaka, A. Oyamada, and M. Takano, *J. Phys. Soc. Jpn.* **65**, 2776 (1996).

¹⁰T. Inami, S. Maegawa, and M. Takano, *J. Magn. Magn. Mater.* **177-181**, 752 (1998).

¹¹Y.-I. Kim and F. Izumi, *J. Ceram. Soc. Jpn.* **102**, 401 (1994).

¹²A. S. Wills and A. Harrison, *J. Chem. Soc., Faraday Trans.* **92**, 2161 (1996).

¹³S.-H. Lee, C. Broholm, M. F. Collins, L. Heller, A. P. Ramirez, C. Kloc, E. Bucher, R. W. Erwin, and N. Lacey, *Phys. Rev. B* **56**, 8091 (1997).

¹⁴A. Harrison, A. S. Wills, and C. Ritter, *Physica B* **241-243**, 722 (1998).

¹⁵A. S. Wills, A. Harrison, S. A. M. Mentink, T. E. Mason, and Z. Tun, *Europhys. Lett.* **42**, 325 (1998).